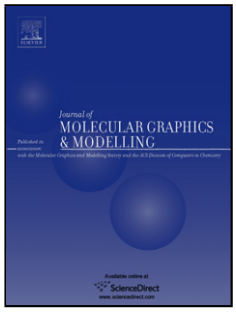

Title: Identification of Novel Allosteric Modulator Binding Sites in NMDA Receptors: A Molecular Modeling Study

Author: Lucas T. Kane Blaise M. Costa

PII: S1093-3263(15)30013-9
DOI: http://dx.doi.org/doi:10.1016/j.jmgm.2015.06.007
Reference: JMG 6561

To appear in: *Journal of Molecular Graphics and Modelling*

Received date: 17-3-2015
Revised date: 16-6-2015
Accepted date: 18-6-2015

Please cite this article as: Lucas T.Kane, Blaise M.Costa, Identification of Novel Allosteric Modulator Binding Sites in NMDA Receptors: A Molecular Modeling Study, Journal of Molecular Graphics and Modelling http://dx.doi.org/10.1016/j.jmgm.2015.06.007

Identification of Novel Allosteric Modulator Binding Sites in NMDA Receptors: A Molecular Modeling Study

Lucas T. Kane[1] and Blaise M. Costa[2]

[1-]Edward Via Virginia College of Osteopathic Medicine, Blacksburg, VA 24060, USA

[2-]Department of Biochemistry, Virginia Polytechnic Institute and State University, Blacksburg VA, 24061, USA; Edward Via College of Osteopathic Medicine, Blacksburg, VA 24060, USA

Corresponding Author

Blaise M. Costa

Assistant Professor

Pharmacology Division

Edward Via College of Osteopathic Medicine

1861 Pratt Drive, Blacksburg, VA

Email: bcosta@vcom.vt.edu

Phone: (540) 231-1468

Fax: (540) 231-8846

Graphical abstract

Highlights

- We generated the 3D models of full length NMDA receptor hetero-tetrameric structures.
- Using subunit selective allosteric modulators we identified four novel binding sites.
- We elucidated the influence of specific amino acid residues within each modulator binding site.
- Our insights contribute for the development of better drugs to treat neurological disorders.

Abstract

The dysfunction of N-methyl-D-Aspartate receptors (NMDARs), a subtype of glutamate receptors, is correlated with schizophrenia, stroke, and many other neuropathological disorders. However, not all NMDAR subtypes equally contribute towards these disorders. Since NMDARs composed of different GluN2 subunits (GluN2A-D) confer varied physiological properties and have different distributions in the brain, pharmacological agents that target NMDARs with specific GluN2 subunits have significant potential for therapeutic applications. In our previous research, we have identified a family of novel allosteric modulators that differentially potentiate and/or inhibit NMDARs of differing GluN2 subunit composition. To further elucidate their molecular

mechanisms, in the present study, we have identified four potential binding sites for novel allosteric modulators by performing molecular modeling, docking, and *in silico* mutations. The molecular determinants of the modulator binding sites (MBS), analysis of particular MBS electrostatics, and the specific loss or gain of binding after mutations have revealed modulators that have strong potential affinities for specific MBS on given subunits and the role of key amino acids in either promoting or obstructing modulator binding. These findings will help design higher affinity GluN2 subunit-selective pharmaceuticals, which are currently unavailable to treat psychiatric and neurological disorders.

Keywords

N-methyl-D-Aspartate receptors (NMDARs); Allosteric Modulators; Molecular Modeling; Docking; Modulator binding sites (MBSs)

Introduction

Neurological disorders affect more than 50 million Americans each year. It is increasingly recognized that many neurological and psychiatric disorders are linked to synaptic defects caused by dysfunction of N-methyl-D-aspartate receptors (NMDARs)[1, 2]. For example, there is evidence for a direct contribution of NMDA receptor dysfunction in stroke damage[3], neuropathic pain[4], Alzheimer's disease[5], Huntington's disease[6], Parkinson's disease[7], traumatic brain injury[8], post-traumatic stress disorder[9], white matter injury[10], autism spectrum disorders[11], depression[12], cognitive impairments[13], schizophrenia[14], epilepsy[15] and anti-NMDA receptor encephalopathy[16]. To date, memantine and ketamine are the only FDA approved drugs that primarily act on the NMDARs and are prescribed for the treatment of moderate to severe Alzheimer's disease [17]. Thus, medications that directly act on NMDARs may have significant therapeutic benefits to these patients [18].

NMDA is an analogue of the excitatory neurotransmitter glutamate that selectively binds with a specific population of glutamate-gated ion channel receptors that are permeable to Ca^{2+}, K^{+} and Na^{+} ions. NMDARs are largely responsible for neuronal plasticity, learning, and memory[19] but cause cell death upon over-activation and psychosis upon hypo-activation. NMDAR isoforms arise from the hetero-tetrameric assembly from seven homologous subunits, GluN1, GluN2A-D, GluN3A&B[20]. Of the four subunits in the receptor complex, two must be GluN1 and the other two can be any combination of GluN2 and/or GluN3 subunits. Thus, there are numerous combinations of di- and tri-heteromeric NMDARs. Physiologically, different combinations of NMDAR channel have distinct properties in terms of agonist affinity, magnesium sensitivity, ion conductance, activation kinetics, open probability, mean open time, cellular localization, and downstream signaling [1, 21]. Thus, as the different GluN subunits have varied distributions in the brain, and different physiological properties, the role of different subtypes of NMDARs in brain function and pathology are also probably quite different from one another. Studies have demonstrated that the activation of extrasynaptic NMDARs (enriched in GluN2B and GluN2D receptors) give signals for brain cell death[22, 23] whereas the activation of synaptic NMDARs (enriched in GluN2A) appears to be pro-survival[2, 24, 25]. These phenomena are poorly understood due to the lack of chemical probes that can distinguish various subunit combinations. These limitations warrant the development of drugs that can better

differentiate NMDARs based on the GluN2 subunit combinations, which would be invaluable for understanding normal brain function and developing improved therapeutics.

All GluN subunits share a similar multi-domain topology containing an N-terminal domain (NTD) and ligand binding domain (LBD) on the extracellular side, a transmembrane domain (TMD) spanning the cell membrane and defining the ion channel pore, and an intracellular carboxyl terminal domain (CTD) within the cytoplasm (Figure 1). The NTD constitutes about 400 amino acids (AAs) that comprise the binding site for endogenous modulators such as Zn^{2+}, polyamines, and protons. The LBD is comprised of ~280 AAs, which is formed by two discontinuous lobes. The first lobe is formed by the AAs between the NTD and transmembrane 1 (M1), and the second is formed by the AAs between M3 and M4. This gives a clamshell-like structure to the LBD enabling NMDARs to tightly bind with the natural agonists (glutamate & glycine) by a Venus fly-trap-like mechanism. The highly conserved TMD is formed by three transmembrane α-helices (M1, M3, and M4) and a membrane-penetrating loop, M2. The CTD is the least conserved domain among all GluN subunits; involved in phosphorylation, membrane trafficking, synaptic localization, activation of second messenger system, and other intracellular interactions [1, 2, 26].

In recent years, the pace of identifying novel drug binding sites on the NMDARs has accelerated, yet only a few sites are well characterized[27]. The first and most well-studied drug binding site in NMDARs is the glutamate binding cleft. This domain is highly conserved and displays about 70-80% AA identity across the GluN2 family. Particularly, AA residues interacting with the ligand are identical in all four GluN2 subunits [28, 29]. Therefore drugs acting on this site are either non-selective or weakly selective (typically 5-10 fold selective) and usually display GluN2A/B selectivity over GluN2C/D for competitive antagonists and the reverse pattern for agonists. At this time, the most selective antagonist that binds at the LBD is 3-(2-carboxypiperazin-4-yl)propyl-1-phosphonic acid (CPP), with a 50-fold selectivity for GluN2A over GluN2D. Conversely, the competitive antagonist (2R*,3S*)-1-(9-bromophenanthrene-3-carbonyl)piperazine-2,3-dicarboxylic acid (UBP145) displays unusual selectivity with a >15 fold selectivity for GluN2D subunit over GluN2A/B, apparently due to occupancy of a distinct site within the glutamate binding cavity[30]. However, this compound is again weakly selective, and the development of more selective compounds is limited by high sequence identity at glutamate binding cleft of GluN2 subunits [30]. Another known drug binding site is in the NTD which was recently co-crystallized with the GluN2B subunit selective allosteric modulator ifenprodil [31, 32]. The third site is formed by the TMD, located at the extracellular vestibule of the ion channel where the endogenous blocker Mg^{2+},[1] and various channel blockers including memantine, MK801 and phencyclidine [33-35] bind.

Recently, by our ongoing efforts to find out GluN2-selective compounds, we discovered a novel family of allosteric modulators that distinguish between NMDARs depending upon their GluN2 subunit composition [21, 36-39]. To date, however, the binding site(s) and mechanisms of action of these compounds still remain unknown. This is partially because of the lack of knowledge about the full-length NMDAR structure that is comprised of a unique, multi-domain patterns of interaction, which was not elucidated until recently by X-ray crystallography. Our previous studies demonstrate that the compounds are not channel blockers, do not bind at the glutamate or glycine binding

sites, and do not require the NTD for their activity[36-38, 40]. Despite the low affinity exhibited by the modulators at this point, their novelty in activity pattern, chemical structure, and mechanism of action warrant further investigation of their binding site with the aim to contribute for the further development of high affinity compounds. This rationale motivated us to investigate the putative binding pockets of the allosteric modulators, as the full-length NMDA receptor x-ray crystallographic structures have been solved recently.

Material & Methods

Model Building

The primary sequences of GluN1 and GluN2A-D subunits were obtained from the NCBI database and analyzed using *BLASTP* program[41]. The multiple sequence alignment of GluN1 and GluN2A-D was done with *Clustal Omega* [42] and was used for determining subunit chains and discerning differences in binding pocket architecture. The X-ray crystal structures of the GluN1/2B full receptor (4PE5[43], 4TLM and 4TLL[44]) were then used as templates to create homology models of the full length NMDARs of GluN1/2A, GluN1/2C, and GluN1/2D using *MODELLER v.9.14*'s spatial restraint method[45]. All the energy minimizations for these models were carried out by the conjugate gradients method. The models were inspected by visualization in *PyMOL* (The PyMOL Molecular Graphics System, Version 1.7.2.1 Schrödinger, LLC.) and the sidechain stereochemistry was evaluated by Ramachandran plots[46] generated by the University of Cambridge's *RAMPAGE* program[47]. The GluN1/2A, C-D models generated from the 4PE5 template are submitted to the *Protein Model Database*[48] and can be located under the following identification numbers: PM0079742 (GluN2A), PM0079774 (GluN2C), and PM0079743 (GluN2D) respectively.

Ligand Preparation

The 3D models of the six novel allosteric modulators (UBP 512, 551, 608, 618, 646, & 710) presented in Costa et al. 2010[37] were obtained using the chemical drawing tool *ChemDraw* (CambridgeSoft). *PRODRG* [49] was then used to generate the required topologies. Each modulator was first prepared using *MGL Tools*[50], a partner program to the molecular docking program *AutoDock Vina*[51], by adding necessary hydrogens and calculating the torsion angles.

Molecular Docking

All ligand docking and scoring was performed by using *AutoDock Vina*. The scoring functions are empirically weighted and contain terms for the values of hydrophobic interactions (van der Waals), hydrogen bonds, and torsion penalties. The search algorithm utilizes an iterated gradient-based local search, in which calculations for a gradient are made while seeking a local optimum. The search space for the ligands was within a 1.7 x 10^6 $Å^3$ size grid box centered at the midpoint of the NMDARs encapsulating the protein. The default number of binding modes (nine) was produced and all were then used in the study due to their accuracy. The exhaustiveness was set to the default (eight) to ensure that there was high probability of the program to find the global minimum of the scoring function. The energy range was set so that there was a maximum energy of 3 kcal/mol between the best and worst binding mode chosen. The resulting docking modes were then used to evaluate the preferred location of binding on each subunit. Whilst AutoDock has shown to be robust and efficient

in finding out the orientations and binding pockets of ligands, particularly with more rigid ligands that contain a small number or no rotatable torsion angles, as in our study (Average of 2.5 torsion angles)[52], there are nonetheless several limiting factors. These limiting factors include the accuracy of force field parameters, limited protein flexibility, simplistic energy functions, and a large search space. The modulators were therefore "blindly docked", which in taking similar limitations into account has still been shown to be a useful technique for the exploration of possible binding sites[52]. Furthermore given their novelty, these findings pave a starting point for otherwise unnoticed MBSs, to explore and validate with experimental techniques in future.

Characterization of the Modulator Binding Sites

Upon identifying the MBSs, *UCSF Chimera*'s [53] "Range" command was used to determine the AAs within 5 Å of the modulators. An important AA was manually selected in each of the four MBSs and mutated using *PyMOL*'s "Mutagenesis" plugin, to either *Ala* or *Gly*. Four mutant receptors were then created for GluN1/2A-D, each with mutations at equivalent locations for MBS-1, 2, 3, and 4. These sixteen models were energy minimized again using the conjugate gradients method within *MODELLER 9.14* and docked using the same methods described above. *PyMOL*'s "Vacuum Electrostatics" plugin was used to examine the electrostatic architecture of MBS-3 by averaging the charges of particular regions of the protein's surface using a quasi-Coulombic-shaped convolution function. The NCBI database numbering is used throughout the study to identify the AAs and the secondary structures are labelled according to the previous crystallographic studies [43, 54].

Results & Discussion

Verification of the Homology Models

Considering that the full-length structures of all GluN2 subunits other than GluN2B are not available, we used homology based modeling to predict their structures. According to *BLASTP*, when compared with the GluN2B subunit, GluN2A, C&D yielded identity scores of 71%, 60%, and 57% respectively. The Ramachandran plot analysis revealed that the GluN2B x-ray crystallographic structure (4PE5), had 93% of its residues in the favored region, and similarly the models generated using 4PE5 as the template had 94%, 93%, and 92% of AAs in the allowed region for GluN1/2A, C&D respectively (Supplementary 1). Furthermore, the models produced by the 4PE5 template displayed observably greater structural integrity, and thus became the template of choice for the entire study (Figure 2a-d). Each model having been improved by the energy minimization procedure was then employed for the molecular docking study.

Analyzing Docking Results

Molecular docking was utilized in order to identify the binding sites of each of the modulators on each of the receptors. The docking results ranked the modes according to their binding energies which represent the sum of the total intermolecular energy, total internal energy, and torsional energy minus the energy of the unbound system (in kcal/mol). To establish a binding score that reflects poor binding, an experimentally known inactive compound, gamma-aminobutyric acid (GABA), was used as the negative control. This compound, consistent with experimental findings, has poor binding scores (average binding energy= -3kcal/mol) when docked with template (4PE5) and the homology models. Therefore, we were able to compare the docking scores

of active UBP compounds with a negative control to validate their binding probability. The average binding energy for all 216 binding modes of UBPs was -8kcal/mol (Supplementary 2), the distinction (-3kcal/mol vs -8kal/mol) between the inactive and active compound binding energies support that the sites of the UBP binding modes are theoretically credible[51]. All nine docking modes identified for each ligand were therefore used and translated to a 0-100% scale (9=100%) to represent the affinity of each modulator. For example, eight out of nine modes (89%) of UBP 710 bound in MBS-1 when docked on GluN1/2B only and an average of 19% of the modes bound in MBS-1 for all other subunits, this distinction corroborate the specificity of UBP 710 to MBS-1 in GluN1/2B. In a similar manner, we analyzed each modulator's binding to specific MBSs of particular subunits of the NMDARs.

Identification of the Four Novel Sites

The docking results revealed that the modulators repeatedly bound with four very specific areas on the NMDARs. In the 4PE5 structure alone, the compounds docked in one of four sites 91% of the time (49 out of 54, total). Overall, 143 (66%) of the modes docked in one of the four novel binding sites (Supplementary 3). The AAs sequences contributing for the structure of the MBSs (Figure 3, Supplementary 4) can be described as follows: MBS-1, located at the back-to-back interface of GluN1/2 LBD, is formed by the C-helix of GluN1 and the I-helix of GluN2 on each side, and then the loop between α-helix 4 and β-sheet 7 acts as the roof. MBS-2 is located at the face to face conformation of the GluN1/2 LBD. The F-helix and the loop between the E and F-helix in the LBD of GluN1 form the base, while the loop between GluN2's β2 and β3 of the LBD, the distal end of α4 in the NTD, and the loop that follows form the top and walls of the MBS-2 pocket. MBS-3 is the only site that is confined to a GluN2 subunit, having no involvement of GluN1 subunit. The pocket appears like a cave with α3 of the NTD, β8, and the loop after β15 forming the back. Then in the LBD, β1 forms the base; while the loop before β3 in LBD, the loop between β3 and β4, and β5 form the sides and ceiling. Remarkably, this binding site has been experimentally validated recently by others for binding with one of their GluN2C selective modulators [55]. Lastly, MBS-4 is formed by the proximal end of α2 of the NTD in both GluN1/2 as well as the small loop between β6 and α4. The predicted binding sites outside of these four MBSs were excluded as they did not meet the acceptable threshold criteria. Primarily, only a low percentage of binding modes docked in such sites (only 28% in the highest case) and secondly the others which bound in the TMD, in addition to low percentage of binding mode, did not have the appropriate structural elements (lipid bilayers) to mimic the native environment of NMDARs.

In-silico Mutagenesis

To validate the influence of specific AAs in the MBS, we introduced the following point mutations; *E188A*, (GluN1), *Y703A* (GluN1), *R392/393/402/415G* (GluN2), and *Y109G* (GluN1) for MBS-1, 2, 3, and 4, respectively (Figure 4a-d). In general, the AAs were selected by analyzing their relative orientation towards the modulator, the chemical nature of their side chain, and their potential role in forming the binding pocket. Specifically, E188 is located at the distal region of NTD and projecting its side chain towards the interface of GluN1/2 interface. The close proximity of this AA side chain to the LBD interface was not known until the availability of full length crystal structure of NMDAR. Consequently, the role of E188 remained unnoticed until

recently. Selecting this AA for mutation in MBS-1 does not conflict with the previous finding that UBP activity is NTD independent; for it can be justified that UBPs may bind with more than one site at a time. Also, in the absence of NTD binding site they can still bind with LBD and give a similar (or some) effect, as observed in the experiments [37]. The AA, Y703 at MBS-2 was chosen for mutation as the orientation of Y703 residue to the modulators appeared to be crucial for forming the binding pocket. Although there are few other AAs located in closer proximity with docked modulators, in order to keep the changes in binding pocket to be common, we avoided GluN2 subunit mutations and selected an AA from GluN1. The MBS-3 mutation was made in the GluN2 subunit since there was no involvement of GluN1 subunit for this MBS. R392 is one of the crucial AAs in the MBS-3 as its side chain is an essential component for forming the backbone of MBS-3. Furthermore, the electropositive chemical nature of the guanidium side chain is critical for providing interaction energy to facilitate modulator binding. In addition, R392 has been found to be crucial for GluN2C specific potentiator binding as identified by a recent experimental study [55]. Lastly, the position of Y109 at MBS-4 is found to be critical because the aromatic sidechain of Y109 creates a pi-stacking interaction with the phenanthrene ring of UBP710, which is imperative for the modulator binding. In order to study the role of this bulky side chain in that position, we have mutated Y109 to glycine, which has a shorter and neutral sidechain.

After virtual mutagenesis, we had 864 different binding modes resulting from the nine modes per modulator on each of the four mutated models for GluN1/2A-D. In order to coherently process this large data set, we individually analyzed the results with regard to the subunits and MBSs, and then the compounds themselves.

Analysis of Modulator Selectivity within GluN1/2A

Analysis of the predicted modulator binding sites provided insights that the compounds exhibit distinct binding properties. Beginning with GluN1/2A, the *Y703A* mutation of the MBS-2 site in the A and C chains of GluN1 greatly reduced the chances of modulator binding. Of the five modulators, which bound to MBS-2 prior to the mutation (UBP 551, 608, 618, 646, and 710), four of them completely lost their binding affinity after *Y703A* mutation (UBP 608, 618, 646, and 710) (Table 1, ★). These results illustrate that the *Y703* residue is critical for promoting binding in MBS-2, particularly when in combination with the GluN2A subunit. These data suggest that the MBS-2 site in GluN1/2A could be a promising therapeutic target for NMDAR site-specific drugs. Additionally the MBS-3 mutation of *R392G* in the B and D chains of GluN2A had the opposite effect in that it secured binding for all six drugs. The only binding inhibition that we observed occurred with UBP 551 (by 11%), conversely this mutation created new binding for UBP 618 and 646 (22% and 56% respectively, Table 1, ●). These data indicate that R392 of GluN2A antagonizes the binding of some modulators at MBS-3; therefore such interactions should be avoided when developing GluN1/2A selective molecules

Analysis of Modulator Selectivity within GluN1/2B&2C

Interestingly, GluN1/2B exhibited a preference towards MBS-1 that was not significantly altered by MBS-1 mutation (Table 1, ■). Prior to the mutations, GluN1/2B docked five of the six compounds in MBS-1 (UBP 512, 551, 608, 646, and 710) and upon mutagenesis five compounds continued to bind in MBS-1, though UBP 618 replaced 608. This suggests that *E188* of the GluN1 A and C chains does not play a significant role in

the modulator's docking in GluN1/2B. In contrast, GluN1/2B and GluN1/2C lost their MBS-3 binding upon GluN1 *R393/402G* mutation; GluN1/2B completely lost binding with UBP 512 and 710, while GluN1/2C lost binding with UBP 551 and 608 (Table 1, ●●). We then used PyMOL's vacuum electrostatics plugin to investigate electrostatic potential differences in the architecture of MBS-3 that contribute to the modulator's selectivity (Figure 5a-d). This data shows that stronger negative electrostatics exist in the center of the MBS-3 pocket for GluN2B and GluN2C (more negative, red) than in the GluN2A&D pocket (more neutral, white). MBS-3 is the only site that does not include an inter-subunit interaction with GluN1, which affirms that the differences between the GluN2A, B, C & D sequences cause these binding disparities. Our electrostatics data in figures 5a-d illustrate how the differences in GluN2 subunit sequences alter the electrostatic environment in their respective binding pockets. This information will be useful for drug developers interested in targeting specific NMDAR subunits to precisely modulate NMDAR activity.

Analysis of Modulator Selectivity within GluN1/2C&2D

Additional mutation/docking results continued to distinguish GluN1/2C and 2D from other the GluN1/2A & 2B complexes as both gained new binding affinities in MBS-4 such that all six compounds bound in this site. As a result of the MBS-4 *Y109G* (GluN1) mutation, five modulators newly bound to MBS-4 for GluN1/2C (UBP 551, 608, 618, 646, and 710) and two for GluN1/2D (UBP 618 and 646) (Table 1, ♦♦). Prior to any mutations these subunits were the only ones in which modulators bound to the MBS-4 site, adding emphasis to the distinct affinity that these compounds have for the GluN2C and GluN2D MBS-4 site. These results demonstrate the importance of *Y109* for the A and C chains of GluN2C and GluN2D for modulator binding. *Y109* proved to be a crucial inhibitor for modulator binding not only for GluN2C&D, but for all subunits. When *Y109* was mutated in MBS-4, it had wider reaching effects than all the other mutations, creating a total of 13 new chances of binding (Table 1, ♦♦♦♦), nearly twice as many as the MBS-1 mutation. Furthermore the mutation at MBS-4 was the only one that did not significantly inhibit a single compound's affinity to bind at this site. Therefore future drugs do not need to be designed to avoid *Y109* interaction if binding in MBS-4 is desired.

GluN1/2D is the only NMDAR to have negligible binding in MBS-2 both before and after the mutation to this site, as only one compound (UBP 646) docked one of its modes with a low probability (11%) (Table 1, ★). This is in stark contrast to all other subunits that bound at least four modulators in this MBS-2 prior to mutations and upon MBS-2 mutation had a total of nine, across all the NMDARs, completely loose binding (Table 1, ★ ★ ★ ★). This provides evidence that *Y703* is a critical AA for increasing affinity towards the binding pocket. Apart from UBP 551 in GluN2A, GluN2D was the only subunit which had no significant changes from any of the MBS mutations for four drugs (UBP 512, 551, 608, and 710). With "significant" being defined as any complete loss of binding, newly created affinity and/or gain/loss of 4 (44%) or more modes of a compound for a specific MBS. Additionally, GluN2D was by far the least affected by the mutations overall with only six significant changes as compared to 13, 12, and 14 significant changes experienced by GluN2A-C respectively (Supplementary 3). Comparison of the strong affinity of compounds for MBS-2 in GluN1/2A to the negligible affinity of that site in GluN1/2D reveals that MBS-2-targeting drugs would have strong enough affinity for MBS-2 of GluN1/2A to have selective binding.

Analysis of the UBP Modulators

By understanding the effects of the novel compounds, the same data can now be analyzed from the perspective of each individual modulator to gain further insight into their subunit selectivity. UBP 512 displays a unique pattern of activity on different population of NMDARs; it has been shown to selectively potentiate GluN2A while inhibiting GluN2C and GluN2D and having no effect on GluN2B [37]. In GluN1/2A, UBP 512 had a distinct affinity for MBS-1 that completely disappeared after *E188A* mutation (Table 1,■). Additionally GluN1/2C & 2D were the only NMDARs to bind UBP 512 in MBS-4 and they were the only subunits to display an inhibitory response to UBP 512 experimentally. This supports the suggestion that modifying UBP 512 to have a greater affinity for MBS-4 would improve its subunit selective inhibitory response on GluN1/2C & 2D. Although UBP 512 activity is largely independent of NTD, we speculate that there could be more than one binding site, and in the absence of one (at NTD) the others may become primary binding site due to the subtle changes in the conformation.

UBP 551 was the only compound that selectively potentiated GluN2D [37]-containing NMDARs. As previously mentioned the mutations in GluN2D did not affect which MBSs bound UBP 551. With these mutations, UBP 551 continued to bind to MBS-1, 3, and 4; the only change being a significant shift of affinity from MBS-1 towards MBS-3 and 4 (Table 1,★). This implies that the AAs selected for mutation were not critical for binding with regard to GluN1/2D. More importantly, UBP 551's affinity for MBS-4 is promising for future selective potentiation considering GluN1/2D stands alone in the degree to which compounds preferred to bind in MBS-4.

UBP 608 selectively inhibits GluN2A-containing NMDARs experimentally [37]. Current modeling suggests that UBP 608 is selective for the MBSs 1, 2, and 3 in GluN1/2A-C (Table 1,●). Additionally, our results show that UBP 608 experienced the greatest overall loss of 4 MBSs after mutations, the vast majority of which occurred in GluN2C. Nearly all binding of UBP 608 was lost in GluN2C; all modes in MBS-1, 2, and 3 were lost while only one mode bound in MBS-4. This suggests that there are strong attractive forces from the chosen AAs in MBS-1, 2, and 3 toward UBP 608 in GluN2A, B&C, but not in GluN2D, which potentially correlates with the minimal inhibitory effects observed in experiments [37].

Despite there being no significant subunit selectivity demonstrated by either UBP 618 or 646, it is still interesting to note that these drugs far surpassed the others in gaining binding modes in the MBSs after mutation. Specifically UBP 618 had an overall gain in binding with 5 more MBSs after mutation, and UBP 646 had an overall gain in binding of 6 MBSs; all of the gains except one coming from MBS-1, 3, and 4 (Table 1,♦ &▲ respectively). This reveals that these two drugs were experiencing severe repulsive effects by the AAs mutated in these MBSs, which indicates that the chemical composition of these compounds do not promote binding in MBS-1, 3, and 4.

UBP 710 selectively potentiates GluN2A or GluN2B containing NMDA receptors expressed in the *xenopus* oocytes [37]. Our results show that UBP 710 has an extremely strong affinity for MBS-1 in GluN2B, which upon mutation at MBS-1 was hardly changed. Additionally the mutation at MBS-1 caused a 67% increase

in the affinity of UBP 710 for GluN2A evidencing that this particular AA plays an opposite role for this modulator's affinity for GluN2A and GluN2B (Table 1,Δ). This indicates that modifying UBP 710 in such a way to have higher affinity for MBS-1 may allow for a more selective potentiation of GluN1/2B alone.

Conclusions

In recent years, many new classes of compounds have emerged that selectively act on NMDARs subunits[27]. Elucidating the mechanisms by which allosteric modulators bind and affect NMDARs function is critical for the further development towards clinical use. The identification of MBS-1 to 4 (in the LBD and NTD portion of the NMDAR) suggests that MBSs are not confined to a specific domain. Moreover, although inter-subunit interfaces are key locations for allosteric regulation, intra-subunit binding sites (MBS-3) are also important regulators of modulator activity. The use of UBP compounds to study NMDAR subunit regulation reveals that, even at highly conserved regions, just a few non-conserved residues can contribute to subunit selectivity. The following findings may serve as useful information for future research on NMDAR binding sites and drug design:

- UBPs with a high affinity for MBS-1 preferentially bind to GluN1/2B.
- Compounds with high affinity for *Y703* (MBS-2) that have a structure similar to UBP 646 and 710, avoid GluN1/2D and prefer GluN1/2A.
- Compounds with a high affinity for MBS-3 not prefer binding in GluN1/2A.
- *Y109* at MBS-4 is antagonist towards modulator binding, therefore compounds avoiding *Y109* will bind MBS-4 more consistently.
- Outstandingly, four of the six UBPs were insignificantly affected by all mutations in GluN1/2D; supporting that there is great possibility for the development of GluN1/2D selective pharmaceutical agents.

Author Contribution

LK did the research work, analyzed data and wrote the manuscript. BMC designed the work, performed, analyzed the data and wrote the manuscript.

Funding

This research work was funded by the Edward Via College of Osteopathic Medicine biomedical research support.

Note: Authors declare no competing financial interest.

Acknowledgments

Authors acknowledge Dr. Dan Monaghan (University of Nebraska Medical Center) and Eryn Perry (Edward Via Virginia College of Osteopathic Medicine) for critical reading of this manuscript. Tara Colquitt (University of Georgia) for the contribution in preparing a figure for this manuscript.

References:

1. Traynelis, S.F., *Glutamate receptor ion channels: structure, regulation, and function.* Pharmacol. Rev., 2010. **62**: p. 405-496.
2. Paoletti, P., C. Bellone, and Q. Zhou, *NMDA receptor subunit diversity: impact on receptor properties, synaptic plasticity and disease.* Nature Rev. Neurosci., 2013. **14**: p. 383-400.
3. Lai, T.W., W.C. Shyu, and Y.T. Wang, *Stroke intervention pathways: NMDA receptors and beyond.* Trends Mol Med, 2011. **17**(5): p. 266-75.
4. Matsumura, S., et al., *Impairment of CaMKII activation and attenuation of neuropathic pain in mice lacking NR2B phosphorylated at Tyr1472.* Eur J Neurosci, 2010. **32**(5): p. 798-810.
5. Kotermanski, S.E. and J.W. Johnson, *Mg2+ imparts NMDA receptor subtype selectivity to the Alzheimer's drug memantine.* J Neurosci, 2009. **29**(9): p. 2774-9.
6. Milnerwood, A.J. and L.A. Raymond, *Early synaptic pathophysiology in neurodegeneration: insights from Huntington's disease.* Trends Neurosci, 2010. **33**(11): p. 513-23.
7. Sgambato-Faure, V. and M.A. Cenci, *Glutamatergic mechanisms in the dyskinesias induced by pharmacological dopamine replacement and deep brain stimulation for the treatment of Parkinson's disease.* Prog Neurobiol, 2012. **96**(1): p. 69-86.
8. Wortzel, H.S. and D.B. Arciniegas, *Treatment of post-traumatic cognitive impairments.* Curr Treat Options Neurol, 2012. **14**(5): p. 493-508.
9. Yamamoto, S., et al., *Effects of single prolonged stress and D-cycloserine on contextual fear extinction and hippocampal NMDA receptor expression in a rat model of PTSD.* Neuropsychopharmacology, 2008. **33**(9): p. 2108-16.
10. Henson, M.A., et al., *Influence of the NR3A subunit on NMDA receptor functions.* Prog Neurobiol, 2010. **91**(1): p. 23-37.
11. Won, H., et al., *Autistic-like social behaviour in Shank2-mutant mice improved by restoring NMDA receptor function.* Nature, 2012. **486**(7402): p. 261-5.
12. Autry, A.E., et al., *NMDA receptor blockade at rest triggers rapid behavioural antidepressant responses.* Nature, 2011. **475**(7354): p. 91-5.
13. Parsons, C.G., A. Stoffler, and W. Danysz, *Memantine: a NMDA receptor antagonist that improves memory by restoration of homeostasis in the glutamatergic system--too little activation is bad, too much is even worse.* Neuropharmacology, 2007. **53**(6): p. 699-723.
14. Moghaddam, B. and D. Javitt, *From revolution to evolution: the glutamate hypothesis of schizophrenia and its implication for treatment.* Neuropsychopharmacology, 2012. **37**(1): p. 4-15.
15. Niimura, M., et al., *Changes in phosphorylation of the NMDA receptor in the rat hippocampus induced by status epilepticus.* J Neurochem, 2005. **92**(6): p. 1377-85.
16. Dalmau, J., et al., *Anti-NMDA-receptor encephalitis: case series and analysis of the effects of antibodies.* Lancet Neurol, 2008. **7**(12): p. 1091-8.

17. Reisberg, B., et al., *Memantine in moderate-to-severe Alzheimer's disease.* N Engl J Med, 2003. **348**(14): p. 1333-41.
18. Marino, M.J. and P.J. Conn, *Direct and indirect modulation of the N-methyl D-aspartate receptor.* Curr Drug Targets CNS Neurol Disord, 2002. **1**(1): p. 1-16.
19. Rebola, N., B.N. Srikumar, and C. Mulle, *Activity-dependent synaptic plasticity of NMDA receptors.* J Physiol, 2010. **588**(Pt 1): p. 93-9.
20. Paoletti, P., C. Bellone, and Q. Zhou, *NMDA receptor subunit diversity: impact on receptor properties, synaptic plasticity and disease.* Nat Rev Neurosci, 2013. **14**(6): p. 383-400.
21. Collingridge, G.L., et al., *The NMDA receptor as a target for cognitive enhancement.* Neuropharmacology, 2013. **64**: p. 13-26.
22. Okamoto, S., et al., *Balance between synaptic versus extrasynaptic NMDA receptor activity influences inclusions and neurotoxicity of mutant huntingtin.* Nat Med, 2009. **15**(12): p. 1407-13.
23. Aluclu, M.U., et al., *Evaluation of effects of memantine on cerebral ischemia in rats.* Neurosciences (Riyadh), 2008. **13**(2): p. 113-6.
24. Hardingham, G.E. and H. Bading, *Coupling of extrasynaptic NMDA receptors to a CREB shut-off pathway is developmentally regulated.* Biochim Biophys Acta, 2002. **1600**(1-2): p. 148-53.
25. Hardingham, G.E. and H. Bading, *Synaptic versus extrasynaptic NMDA receptor signalling: implications for neurodegenerative disorders.* Nat Rev Neurosci, 2010. **11**(10): p. 682-96.
26. Sun, Y., *Mechanism of glutamate receptor desensitization.* Nature, 2002. **417**: p. 245-253.
27. Zhu, S. and P. Paoletti, *Allosteric modulators of NMDA receptors: multiple sites and mechanisms.* Curr Opin Pharmacol, 2014. **20C**: p. 14-23.
28. Kinarsky, L., et al., *Identification of subunit- and antagonist-specific amino acid residues in the N-Methyl-D-aspartate receptor glutamate-binding pocket.* J Pharmacol Exp Ther, 2005. **313**(3): p. 1066-74.
29. Blaise, M.C., et al., *Evolutionary trace analysis of ionotropic glutamate receptor sequences and modeling the interactions of agonists with different NMDA receptor subunits.* J Mol Model, 2004. **10**(5-6): p. 305-16.
30. Costa, B.M., et al., *N-methyl-D-aspartate (NMDA) receptor NR2 subunit selectivity of a series of novel piperazine-2,3-dicarboxylate derivatives: preferential blockade of extrasynaptic NMDA receptors in the rat hippocampal CA3-CA1 synapse.* J Pharmacol Exp Ther, 2009. **331**(2): p. 618-26.
31. Williams, K., *Ifenprodil discriminates subtypes of the N-methyl-D-aspartate receptor: selectivity and mechanisms at recombinant heteromeric receptors.* Mol Pharmacol, 1993. **44**(4): p. 851-9.
32. Karakas, E., N. Simorowski, and H. Furukawa, *Subunit arrangement and phenylethanolamine binding in GluN1/GluN2B NMDA receptors.* Nature, 2011. **475**(7355): p. 249-53.
33. Bormann, J., *Memantine is a potent blocker of N-methyl-D-aspartate (NMDA) receptor channels.* Eur J Pharmacol, 1989. **166**(3): p. 591-2.
34. Wong, E.H., et al., *The anticonvulsant MK-801 is a potent N-methyl-D-aspartate antagonist.* Proc Natl Acad Sci U S A, 1986. **83**(18): p. 7104-8.
35. Anis, N.A., et al., *The dissociative anaesthetics, ketamine and phencyclidine, selectively reduce excitation of central mammalian neurones by N-methyl-aspartate.* Br J Pharmacol, 1983. **79**(2): p. 565-75.
36. Costa, B.M., et al., *Structure-activity relationships for allosteric NMDA receptor inhibitors based on 2-naphthoic acid.* Neuropharmacology, 2012. **62**(4): p. 1730-6.
37. Costa, B.M., et al., *A novel family of negative and positive allosteric modulators of NMDA receptors.* J Pharmacol Exp Ther, 2010. **335**(3): p. 614-21.

38. Irvine, M.W., et al., *Coumarin-3-carboxylic acid derivatives as potentiators and inhibitors of recombinant and native N-methyl-D-aspartate receptors.* Neurochem Int, 2012. **61**(4): p. 593-600.
39. Monaghan, D.T., et al., *Pharmacological modulation of NMDA receptor activity and the advent of negative and positive allosteric modulators.* Neurochem Int, 2012. **61**(4): p. 581-92.
40. Irvine, M.W., et al., *Piperazine-2,3-dicarboxylic acid derivatives as dual antagonists of NMDA and GluK1-containing kainate receptors.* J Med Chem, 2012. **55**(1): p. 327-41.
41. Gish, W. and D.J. States, *Identification of protein coding regions by database similarity search.* Nat Genet, 1993. **3**(3): p. 266-72.
42. Sievers, F., et al., *Fast, scalable generation of high-quality protein multiple sequence alignments using Clustal Omega.* Mol Syst Biol, 2011. **7**: p. 539.
43. Karakas, E. and H. Furukawa, *Crystal structure of a heterotetrameric NMDA receptor ion channel.* Science, 2014. **344**(6187): p. 992-7.
44. Lee, C.H., et al., *NMDA receptor structures reveal subunit arrangement and pore architecture.* Nature, 2014. **511**(7508): p. 191-7.
45. Sali, A. and T.L. Blundell, *Comparative protein modelling by satisfaction of spatial restraints.* J Mol Biol, 1993. **234**(3): p. 779-815.
46. Ramachandran, G.N., C. Ramakrishnan, and V. Sasisekharan, *Stereochemistry of polypeptide chain configurations.* J Mol Biol, 1963. **7**: p. 95-9.
47. Lovell, S.C., et al., *Structure validation by Calpha geometry: phi,psi and Cbeta deviation.* Proteins, 2003. **50**(3): p. 437-50.
48. Castrignano, T., et al., *The PMDB Protein Model Database.* Nucleic Acids Res, 2006. **34**(Database issue): p. D306-9.
49. Schuttelkopf, A.W. and D.M. van Aalten, *PRODRG: a tool for high-throughput crystallography of protein-ligand complexes.* Acta Crystallogr D Biol Crystallogr, 2004. **60**(Pt 8): p. 1355-63.
50. Sanner, M.F., *Python: a programming language for software integration and development.* J Mol Graph Model, 1999. **17**(1): p. 57-61.
51. Trott, O. and A.J. Olson, *AutoDock Vina: improving the speed and accuracy of docking with a new scoring function, efficient optimization, and multithreading.* J Comput Chem, 2010. **31**(2): p. 455-61.
52. Hetenyi, C. and D. van der Spoel, *Efficient docking of peptides to proteins without prior knowledge of the binding site.* Protein Sci, 2002. **11**(7): p. 1729-37.
53. Pettersen, E.F., et al., *UCSF Chimera--a visualization system for exploratory research and analysis.* J Comput Chem, 2004. **25**(13): p. 1605-12.
54. Furukawa, H. and E. Gouaux, *Mechanisms of activation, inhibition and specificity: crystal structures of the NMDA receptor NR1 ligand-binding core.* EMBO J, 2003. **22**(12): p. 2873-85.
55. Khatri, A., et al., *Structural determinants and mechanism of action of a GluN2C-selective NMDA receptor positive allosteric modulator.* Mol Pharmacol, 2014. **86**(5): p. 548-60.

Fig 1 All GluN subunits share the similar structure which is composed of four distinct domains: an N-terminal domain (NTD), a ligand binding domain (LBD) that binds to glycine or D-serine in GluN1 (light brown) subunit and glutamate in GluN2 (maroon) subunit, a transmembrane domain (TMD) spanning the cell membrane and defining the ion channel pore, and an intracellular carboxyl terminal domain (CTD) within the cytoplasm. The LBD is formed by two discontinuous lobes, the amino acids (AAs) between NTD and transmembrane 1 (M1) contribute for lobe one, and the AAs between M3 and M4 form lobe two. These two lobes form a clamshell-like structure that enables NMDA receptors to tightly bind with the natural agonists (glutamate & glycine) by the venous fly-trap mechanism.

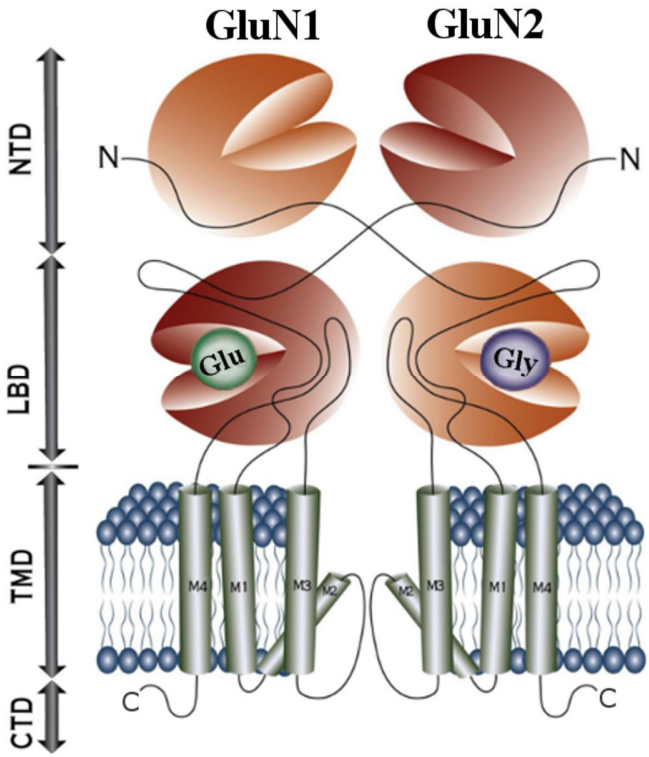

Fig 2 Pictures showing the homology models of GluN1/2A (a),GluN1/2C (c), GluN1/2D (d) generated using MODELLER v.9.14 with the X-ray crystal structure of GluN1/2B (b) (PDB: 4PE5) as the template. GluN1 subunits are yellow while the GluN2A-D subunits are red, blue, green, and magenta respectively. Compared with the GluN2B subunit, GluN2A, C-D yielded percentage sequence identity scores of 71%, 60%, and 57% respectively. The lower amino acid sequence identity for GluN1/2C-D with the template gives reason for the slight bend in the TMD.

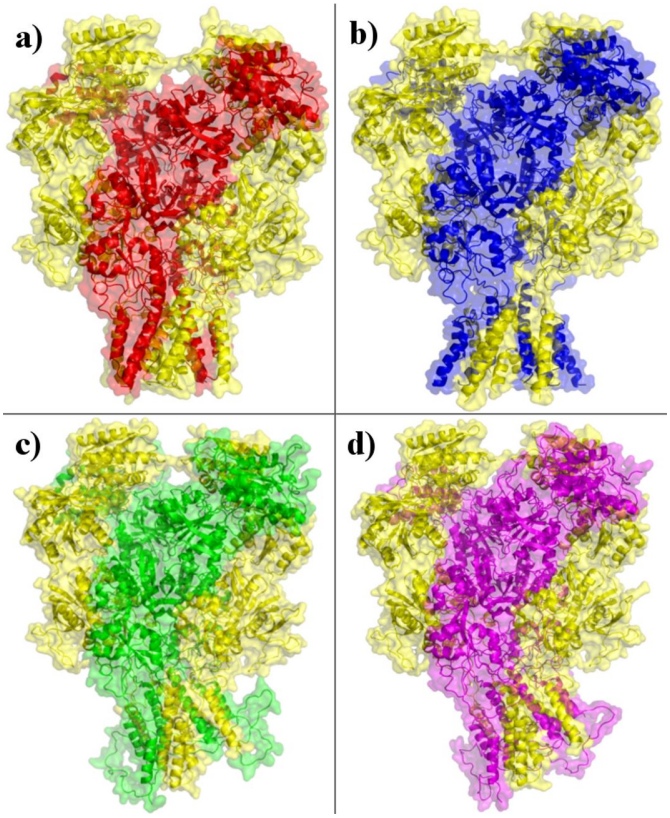

Fig 3 The multiple sequence alignment of GluN1 and GluN2A-D are depicted with α-helices (cylinder shape) and β-sheets (arrowhead) in orange and maroon representing the ligand binding domain (LBD) and N-terminal domain (NTD) respectively. The secondary structures are marked only when that specific region is contributing for the modulator binding site (MBS) for all five subunits (GluN1, 2A-D) and are labelled according to previous crystallographic studies [43, 54]. The sequence segments displayed are those that play a key role in forming the pocket for each MBS. The AAs within a 5 Å range of each MBS are colored in a subunit specific manner; red, blue, green, and magenta representing GluN2A-D respectively. The AAs chosen for mutation in each MBS are identified by the red boxes, while the black boxes are to indicate the AAs within the 5 Å range that are different between specific subunits. See Supplementary 4 for more details.

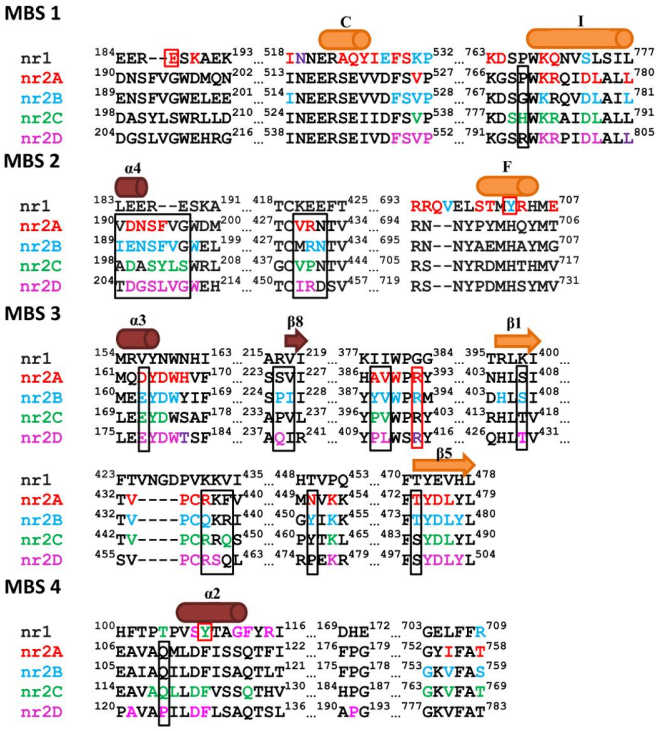

Fig 4 The picture shows the novel MBSs on the GluN1 (yellow)/2A (red) receptor, as representatives for the other subunits. The location of MBS 1-4 are labeled in the full length NMDAR picture. The polypeptide chains forming the binding pocket are in cartoon and the others are depicted as transparent molecular surface. UBP 710 was chosen as the example docked modulator and is depicted as transparent spheres in all four sites. The AAs within a 5Å range of the modulators are grey and in stick. AAs marked in green are those selected for mutagenesis: *E188A* of A-chain/C-chain, (GluN1)*; Y703A* of A-chain/C-chain; *R392G* of B-chain/D-chain, (GluN2); and *Y109G* of the A-chain/C-chain, for MBS 1-4 respectively. MBS-1, located at the "back-to-back" interface of GluN1/2 LBD, creates slots for the modulators to bind with the C-helix of GluN1 and the I-helix of GluN2 on each side, and then the loop between α-helix 4 and β-sheet 7 forming the roof. MBS-2 is located at the "face-to-face" conformation of the GluN1/2 LBD. The F-helix and the loop between it and the E-helix in the LBD of GluN1 form the base, while the distal end of α4 in the NTD and the loop that follows form the roof and sides of the MBS-2 pocket. MBS-3 is the only site that is confined to a GluN2 subunit, having no involvement of GluN1 subunit. The pocket appears like a groove with α3 of the NTD, β8, and the loop after β15 forming one side. Then β1 of the LBD forms the base; while the loop before β3 in LBD, the loop between β3 and β4, and β5 form the other sides and roof. Lastly, MBS-4 is formed by the proximal end of α2 of the NTD in both GluN1/2 as well as the small loop between β6 and α4.

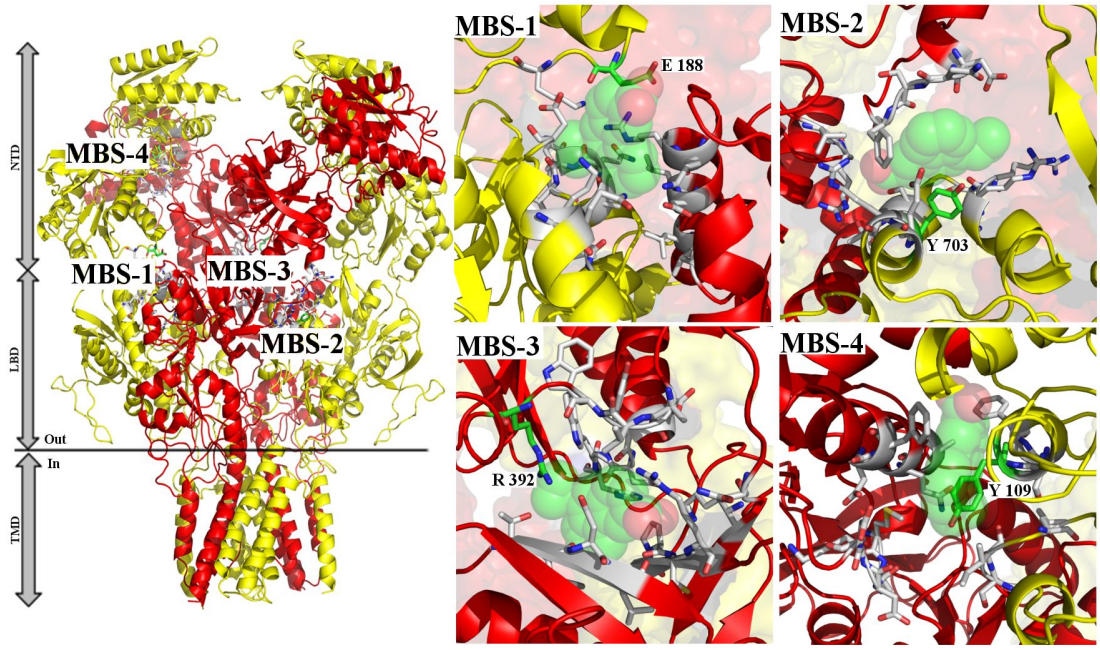

Fig 5 The surface electrostatics of the MBS-3 in all four GluN2 subunits. The electrostatic properties are marked by white (neutral), blue (positive), and red (negative); in PyMOL the color slider was set within ± 0.100 of ± 70.500 (K_bT/e_c). The B chain of each GluN2 subunit is shown (a-d), and zoomed in on the center of MBS-3. Upon observation it is evident that the center of both GluN2B&C (b & c) have unique negative electrostatics (red regions) whereas GluN2A&D (a & d) do not.

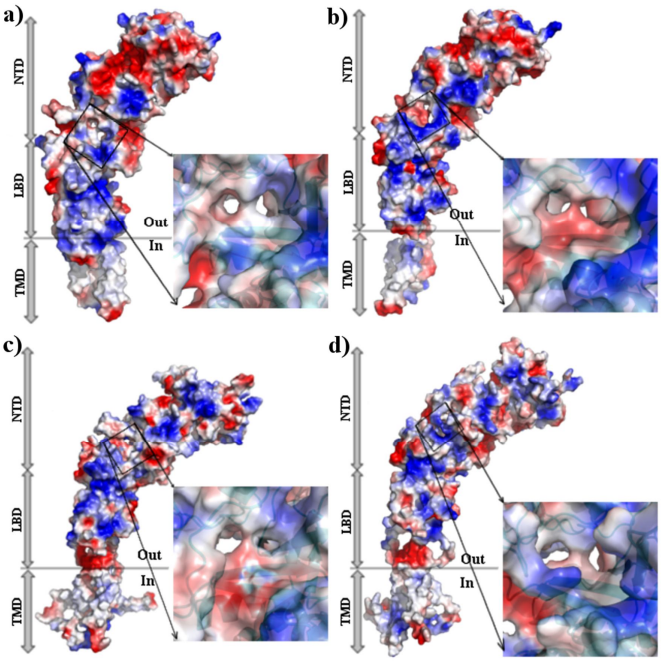

Table 1 The docking results are color coordinated using red, blue, green, and magenta to distinguish GluN2A-D respectively. The five columns following the GluN subunits represent the four MBSs and the six modulators (UBPs). The AAs are labeled according to the NCBI database numbering. The data scores are based on the number

of modes that bound in a pocket with the highest possible being nine and have been translated to percentages (9=100%). The variable green shades are correlated to the percentages to illustrate the probability of binding for an MBS; white being the least likely and dark green the most. The third set of columns illustrate the losses or gains of binding chances after mutation in each subunit and MBS. For any notable findings within MBS 1-4, the following shapes are used respectively, ■, ★, ●, and ♦ ; and colored with the correlating GluN2 subunit. To summarize the results of the UBPs, the modulators were represented by the following shapes: ■ (512), ★ (551), ● (608), ♦ (618), ▲ (646), and Δ (710) were used.

Docking						Docking After Point Mutation						Loss and Gain of Docking Score					
GluN	MBS-1	MBS-2	MBS-3	MBS-4	UBP	GluN	MBS-1 GluN1 (E188A)	MBS-2 GluN1 (Y703A)	MBS-3 GluN2 (R392/393/ 402/415G)	MBS-4 GluN1 (Y109G)	UBP	GluN	MBS-1 GluN1 (E188A)	MBS-2 GluN1 (Y703A)	MBS-3 GluN2 (R392/393/ 402/415G)	MBS-4 GluN1 (Y109G)	UBP
2A	44	0	11	0	512	2A	0	33	22	11	512	2A	-44	33	11	11	512
	33	11	22	0	551		22	11	11	0	551		-11	0	-11	0	551
	44	22	22	0	608		33	0	44	0	608		-11	-22	22	0	608
	0	22	0	0	618		11	0	22	0	618		11	-22	22	0	618
	0	33	0	0	646		11	0	56	56	646		11	-33	56	56	646
	11	33	33	0	710		78	0	33	22	710		67	-33	0	22	710
2B	33	33	33	0	512	2B	56	0	0	0	512	2B	23	-33	-33	0	512
	44	0	44	0	551		22	22	33	11	551		-22	22	-11	11	551
	22	33	33	0	608		0	11	44	0	608		-22	-22	11	0	608
	0	44	22	0	618		22	11	33	33	618		22	-33	11	33	618
	11	33	56	0	646		44	0	33	22	646		33	-33	-23	22	646
	89	0	11	0	710		67	0	0	0	710		-22	0	-11	0	710
2C	0	11	11	22	512	2C	22	0	11	33	512	2C	22	-11	0	11	512
	0	0	67	0	551		0	0	0	11	551		0	0	-67	11	551
	22	22	33	0	608		0	0	0	11	608		-22	-22	-33	11	608
	0	22	11	0	618		0	22	11	22	618		0	0	0	22	618
	0	22	0	0	646		0	67	11	33	646		0	45	11	33	646
	44	0	11	0	710		33	11	33	33	710		-11	11	22	33	710
2D	0	0	0	67	512	2D	0	0	0	33	512	2D	0	0	0	-34	512
	44	0	11	22	551		11	0	78	78	551		-33	0	67	56	551
	0	0	22	44	608		0	0	11	22	608		0	0	-11	-22	608
	11	0	78	0	618		56	0	78	67	618		45	0	0	67	618
	0	11	11	0	646		0	0	11	33	646		0	-11	0	33	646
	0	0	67	11	710		0	0	33	44	710		0	0	-34	33	710